

Laser-induced ultrafast dynamics in C₆₀

G. P. Zhang

Department of Physics, Indiana State University, Terre Haute, Indiana 47809, USA

X. Sun

Department of Physics, Fudan University, Shanghai 200433, China

Thomas F. George

Office of the Chancellor and Departments of Chemistry & Biochemistry and Physics & Astronomy, University of Missouri-St. Louis, St. Louis, Missouri 63121, USA

(Received 15 April 2003; revised manuscript received 16 June 2003; published 20 October 2003)

When a laser shines on C₆₀, electrons are initially excited out of the occupied states, and the laser energy is mainly absorbed into the electron system. After the laser pulse is over, the lattice and the electron systems start to exchange energy periodically. A time-dependent density-matrix simulation reveals that depending on the incident laser frequency and pulse duration, the absorbed energy exhibits a higher-order dependence on the field amplitude, consistent with the experimental findings. Interestingly, due to the Stark effect, on resonance the absorbed energy may decrease with an increase in the field amplitude, which is important for future optical limiting applications.

DOI: 10.1103/PhysRevB.68.165410

PACS number(s): 78.66.Tr, 42.65.Re, 36.40.Vz

I. INTRODUCTION

With its unique structure, C₆₀ exhibits an extremely fast response upon laser excitation.¹ Early experiments showed that relaxation occurs on a picosecond time scale,² and with improved laser resolution, the intrinsic relaxation time was shown to be shorter than 100 fs.³ This is promising for ultrafast optical switching and optoelectronic gates. Sariciftci *et al.*⁴ fabricated a prototype C₆₀/polymer diode,⁵ while Kraabel *et al.* and recently Lanzani⁶ found that charge transfer from semiconducting polymers to C₆₀ occurs within 50 fs. As is well known, such a fast response is often a good indication of a strong nonlinear optical effect. Kafafi *et al.*⁷ reported a third-order susceptibility off resonance up to 7×10^{-12} esu (electrostatic unit⁸) at 1064 nm and observed a fifth-order contribution at higher laser intensities. Tutt and Kost⁹ demonstrated optical limiting in C₆₀ solution, with a saturation threshold equal to or lower than those of the optical-limiting materials currently in use.¹⁰

These and other exciting experimental results have motivated many theoretical studies. It has been shown that upon laser irradiation, the system will undergo a symmetry reduction from I_h to D_{5d} or D_{3d} .¹¹⁻¹⁴ A dynamical simulation shows that after photoexcitation, electrons quickly become self-trapped,¹³ and the bond structure develops into a polaronic shape.¹⁴ These simulations were able to reproduce the correct order of magnitude of the relaxation time. One feature of these previous simulations is that they normally do not include the laser field explicitly and treat the dynamics as a dark evolution. In other words, the laser excitation is implicitly incorporated through 'promoting' electrons out of the highest occupied molecular orbitals (HOMO) into the lowest unoccupied molecular orbitals (LUMO). This technique is very straightforward and has been widely used in the literature, in particular for conjugated polymers such as polyacetylene,¹⁵ but a direct comparison with experiments is

difficult as the laser field may substantially affect the dynamics.¹⁶ Moreover, in C₆₀ there is an additional difficulty. Since its HOMO (H_{1u}) and LUMO (T_{1u}) both have ungerade symmetry, rigorously speaking, a direct transition from HOMO to LUMO is dipole forbidden. Therefore, a direct comparison with experimental results becomes even more difficult for C₆₀, if not impossible.

In this paper, we include the laser field realistically and employ the density-matrix formalism, which gives us full flexibility to simulate the ultrafast dynamics. Initially, the laser frequency is tuned to excite the first dipole-allowed transition from HOMO to LUMO+1. As electrons are excited out of the occupied orbitals, the electron-phonon coupling results in the original fivefold degenerate H_u states localized in the wells of E_{1u} , E_{2u} , and A_{1u} , and the T_{1g} states in the wells of E_{1g} and A_{2g} . The laser energy is first absorbed into just the electron subsystem. After the laser pulse is over, the electron subsystem swaps energy with the lattice subsystem. Our simulation shows that the experimentally observed high-order nonlinearity at higher laser intensities sensitively depends on the laser pulse duration and frequency. In particular, on resonance the total absorbed energy may decrease with an increase in the laser intensity. This could be useful for optical limiting applications.

The paper is arranged as follows. In Sec. II, we present the theoretical algorithm and results. In Sec. III, a comparison with experiments is provided. Finally, we provide concluding remarks in Sec. IV.

II. THEORETICAL SCHEME AND RESULTS

C₆₀ has the I_h point symmetry. Neutral C₆₀ has 60 π electrons, where its interball hopping is very small compared with the on-ball hopping and therefore is neglected here. The Hamiltonian for the whole system can then be written as¹⁴

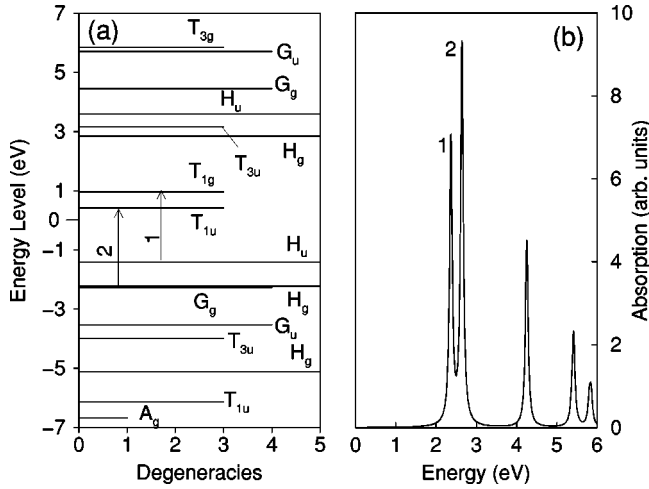


FIG. 1. (a) Energy levels vs degeneracy for C_{60} . Below 0 eV, all states are occupied. (b) Absorption spectrum. The first peak corresponds to the first dipole-allowed transition in (a) from HOMO (H_u) to LUMO+1 (T_{1g}).

$$H_0 = - \sum_{i,j,\sigma} t_{ij} (c_{i,\sigma}^\dagger c_{j,\sigma} + \text{H.c.}) + \frac{K}{2} \sum_{i,j} (r_{ij} - d_0)^2, \quad (1)$$

where $c_{i,\sigma}^\dagger$ is the electron creation operator at site i with spin $\sigma (= \uparrow \downarrow)$.^{17,18} The first term on right-hand side (RHS) represents the electron hopping, where $t_{ij} = t^0 - \alpha(|\mathbf{r}_i - \mathbf{r}_j| - d_0)$ is the hopping integral between nearest-neighbor atoms at \mathbf{r}_i and \mathbf{r}_j , and $r_{ij} = |\mathbf{r}_i - \mathbf{r}_j|$. Here t^0 is the average hopping constant, α is the electron-lattice coupling constant, and d_0 is the carbon-carbon bond length in diamond which is 1.54 Å. The second term on the RHS is the lattice elastic energy, where K is the spring constant. By fitting the energy gap and bond lengths, we have determined the above parameters as $t^0 = 1.8$ eV, $\alpha = 3.5$ eV/Å, and $K = 30.0$ eV/Å² (see Ref. 14).

For an unexcited C_{60} , we compute the energy level scheme by directly diagonalizing the electronic part of the Hamiltonian in Eq. (1). Figure 1(a) shows the energy levels vs degeneracies. The levels below 0 eV (Fermi level) are all occupied, and above it they are all unoccupied. The first dipole-allowed transition is from H_u to T_{1g} [see the arrow labeled by 1 in Fig. 1(a)], which leads to the first peak at $E_1 = 2.37$ eV in the optical absorption spectrum in Fig. 1(b). Since we are mainly interested in the excitation around the Fermi level, from here on, when we mention T_{1g} , T_{1u} , H_u , and H_g , we always refer to those levels close to the zero energy in Fig. 1(a).

Different from many previous investigations,^{14,19} we realistically and systematically include the laser field, which is described by

$$H_I = -e \sum_{i\sigma} \mathbf{E}(t) \cdot \mathbf{r}_i n_{i\sigma}, \quad (2)$$

where $|\mathbf{E}(t)| = A \cos(\omega(t-t_0)) \exp[-(t-t_0)^2/\tau^2]$ (Ref. 20). Here A is the amplitude of the field, ω is the laser frequency, τ is the pulse duration or width, e is the electron charge, t is the time, and t_0 is the time delay.²¹ To describe the time-

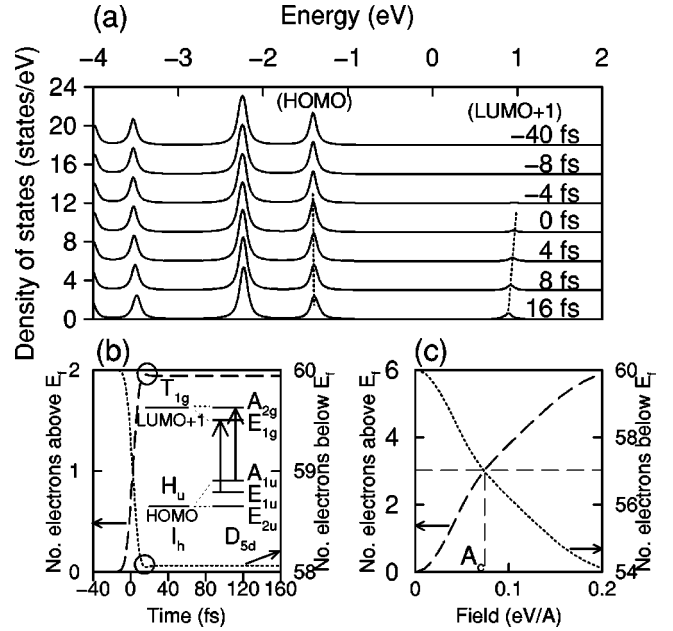


FIG. 2. (a) Density of states as a function of energy at different times. The dashed lines highlight the shifts of the energy levels. (b) The total electron number change in the states above (long-dashed line) and below (dotted line) the Fermi level, where the left (right) y axis should be used, respectively. (Inset) The symmetry is reduced from I_h to D_{5d} , and the original degenerate levels are split into several levels with reduced degeneracies. (c) Change of the total number of electrons with the field amplitude. The long-dashed and dotted lines have the same meanings as those in (b).

dependent ultrafast dynamics, we numerically solve the equation of motion for the electron density matrices,²⁰

$$-i\hbar \frac{\partial \rho_{ij\sigma}}{\partial t} = \langle [\rho_{ij\sigma}, H] \rangle, \quad (3)$$

where $H = H_0 + H_I$, and the density matrix is $\rho_{ij\sigma} = \langle c_{i\sigma}^\dagger c_{j\sigma} \rangle$. The density-matrix formalism is advantageous over the scheme with fixed electron filling since it allows for fractional electron occupations and enables us to investigate the electron number change upon laser excitation. We treat the carbon atom classically by solving the Newton dynamical equation.^{14,22}

We use a laser pulse with duration $\tau = 10$ fs, field magnitude $A = 0.05$ eV/Å, frequency $\omega = E_1 = 2.37$ eV exactly at the first absorption peak in Fig. 1(b), and time delay $t_0 = 0$.²¹ Initially, the lattice is in its equilibrium, and all the 60 electrons occupy those 30 lowest energy levels with the rest of levels unoccupied. Upon laser excitation, electrons are first excited. Figure 2(a) shows that the density of states (DOS) changes with time at the very early stages. At $t = -40$ fs, the laser pulse has not arrived yet, and the corresponding curve represents the normal C_{60} DOS, where the highest energy peak comes from the H_u state (HOMO) and the second peak from the H_g and G_g states. At $t = -8$ fs,²¹ the whole system is already driven by the laser field since the duration is 10 fs,²¹ but there is no sizable DOS change. However, at $t = -4$ fs the DOS starts to shake up, and a very small hump

appears slightly below 1 eV in the (LUMO+1). This hump increases in amplitude while its position shifts to the lower energy side. In the meantime, a drop in the DOS of the HOMOs can be noted, but its position shifts slightly toward the high energy side. We highlight these changes by the dashed lines. Underlying these energy shifts is the splitting of the T_{1g} and H_u states. Due to the electron-phonon coupling,¹¹ T_{1g} is split into E_{1g} and A_{2g} , and H_u into A_{1u} , E_{1u} , and E_{2u} [see the inset in Fig. 2(b)]. In other words, the electron-phonon coupling results in T_{1g} and H_u states localized in the wells of the reduced symmetry states, [E_{1g} and A_{2g}] and [A_{1u} , E_{1u} , and E_{2u}], respectively. Tunneling among these wells is weak, thus the restoration of the original symmetry is not possible until both lattice and electron cool down to the ground state. We find these states are not equally populated or vacated. For instance, A_{2g} gains 0.73 electron and the two E_{1g} gain about 0.60 electron each, while the A_{1u} state loses about 0.73 electron, the two E_{1u} lose 0.60 each, and the two E_{2u} are dark states and are virtually unaffected. This suggests that the electronic transition may proceed in a two-channel fashion [see the two arrows in Fig. 2(b)]. We caution that while the group theory gives the splittings of these levels, the ordering of these levels in the inset of Fig. 2(b) may change with time, and the two-channel transition is a numerical result.²³

The total electron number change as a function of time is shown in Fig. 2(b). The long-dashed (dotted) line denotes the total number of electrons in the states above (below) the Fermi level, where the left (right) y axis should be used. We see that at $t=0$ fs, approximately one electron is pumped out of the HOMOs and into the LUMOs. The change reaches its maximum of about two electrons around 16 fs. There is a small peak which is highlighted with small circles. We can verify that this peak originates from the lattice vibration by switching off the lattice. After 16 fs, the total occupation change is complete.

Figure 2(c) shows the total electron number change in the long-time limit vs the field amplitude, where the laser frequency and pulse duration are the same as above. Similarly, the long-dashed and dotted lines have the same meanings as those in Fig. 2(b). One can see that a stronger field sharply increases the number of electrons excited. But once the amplitude is larger than $A_c=0.067$ eV/Å, the increase slows down and becomes slightly saturated. The reason for such a saturation is due to the well-known Pauli blocking effect (or state-filling effect) as frequently seen in semiconductors.²⁴ At A_c , the total electron number change is three, which corresponds to the half-filling of the threefold degenerate T_{1g} (LUMO+1) state. Due to the Pauli exclusion principle, once some of the energy levels are filled, the number of available channels diminishes, and any additional filling has to go to other levels, which blocks further electron promotions. The fact that T_{1g} can accommodate six electrons in total explains why the occupations still increase with the laser intensity after A_c , but the blocking effect becomes stronger with an increase of the occupation, which ultimately leads to population saturation around $A=0.2$ eV/Å. Such a saturation effect is a nice optical analog to the transport problem, where the current-voltage (I-V) curve shows a flat step each time an

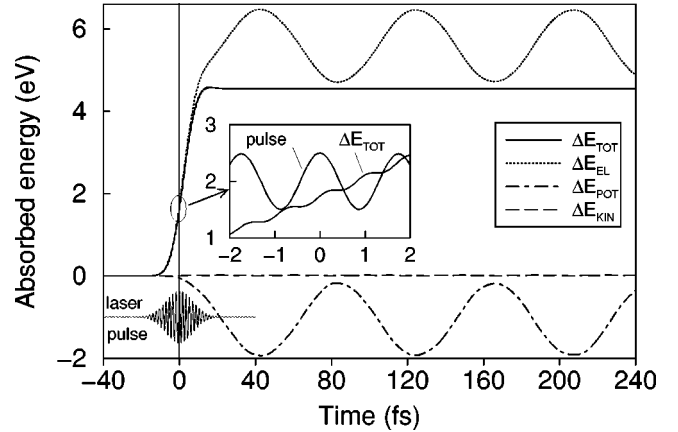


FIG. 3. Absorbed energy vs time. The total absorbed energy change ΔE_{TOT} , electron energy change ΔE_{EL} , lattice potential energy change ΔE_{POT} and kinetic energy change ΔE_{KIN} are denoted by the solid, dotted, dot-dashed, and long-dashed lines, respectively. The laser pulse is shown in the lower left corner. In a small window around 0 fs, the change of ΔE_{TOT} is shown in the middle inset, together with the rescaled pulse shape.

energy level is filled.²⁵ We should stress that such a nice relation between the occupation change and the laser intensity is not possible to investigate within the previous formalism, where the occupation of energy levels is fixed from the beginning. This demonstrates the beauty of the density-matrix formalism.

The change of electron occupation certainly leads to the system's energy change. Figure 3 shows how the laser energy is absorbed into the system, where the field amplitude is still 0.05 eV/Å and the other parameters are the same as those in Fig. 2(a). The x axis denotes the time in units of femtosecond, while the y axis represents the energy change with respect to the original energy of the unexcited system. The thick solid line denotes the total energy change ΔE_{TOT} , the dotted line represents the total electron energy change ΔE_{EL} , the dot-dashed line shows the total lattice potential energy change ΔE_{POT} , and the kinetic energy change ΔE_{KIN} is denoted by the long dashed line. At first we focus on ΔE_{TOT} . One sees that upon laser excitation, ΔE_{TOT} increases sharply and closely follows the shape of the laser pulse, which is shown in the lower left corner. While ΔE_{TOT} continues to increase, it becomes slightly overheated around 16 fs. After 20 fs, ΔE_{TOT} settles down at about 4.54 eV. From Fig. 2(b), we know that the total number of electrons is about 1.94, so that each electron acquires 4.54 eV/1.94, i.e., 2.34 eV, which is almost exactly equal to the energy gap between the new HOMO and LUMO+1 states. To see more clearly how the energy has been absorbed into the system at an earlier stage, we enlarge a small portion around 0 fs (see the elliptic circle) and show ΔE_{TOT} in the middle inset, where the x and y axes are the same as in the full figure. We rescale the laser pulse's amplitude and superimpose it on top of ΔE_{TOT} . It is interesting to see that the system absorbs the energy in an oscillatory fashion, with a period almost half of the external laser field.

After 20 fs, although ΔE_{TOT} does not change, its components do. At the beginning of excitation, the absorbed energy

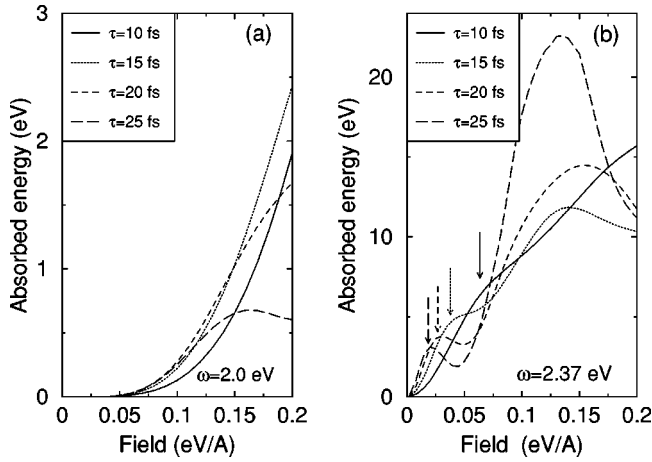


FIG. 4. Total absorbed energy vs laser field amplitude for different laser pulse durations for (a) off resonant and (b) resonant excitations.

almost exclusively enters the electron subsystem, while the lattice gains no energy (see the dot-dashed line just before 0 fs). After 0 fs, however, the change in the lattice energy becomes obvious, with a major change in the potential energy ΔE_{POT} and a very small change in the kinetic energy ΔE_{KIN} . We notice that ΔE_{POT} is always negative in our present case, indicating that the lattice loses energy, but ΔE_{EL} gains more than the energy lost by the lattice. Thus, the system as a whole still has a net gain in energy from the laser field. After the laser pulse is over, ΔE_{POT} and ΔE_{EL} oscillate periodically out of phase. The period of the oscillation is about 83.8 fs,²⁶ which is close to the experimental value of 67 fs.³ This oscillation originates from the well-known A_g radial breathing mode.²⁷

III. COMPARISON WITH EXPERIMENTS

Experimentally, Kafafi *et al.*⁷ found evidence for a fifth-order contribution to the nonlinear optical response at high laser intensities, but their fixed laser wavelength prevented them from investigating this problem systematically. Here, by including the laser field, we can effectively address the problem. Our numerical simulation shows that the real picture is extremely rich. Note that the absorbed energy is a direct measure of the system's polarizability. Thus, studying the absorbed energy will reveal similar information.

We begin with an off-resonant case as done experimentally. The laser frequency is tuned to $\omega = 2.0$ eV, which is far below the first resonance. In Fig. 4(a), we show the absorbed energy ΔE_{TOT} in the long-time limit as a function of the field amplitude A for different pulse durations or widths τ . One notices that if $\tau = 10$ fs, the absorbed energy superlinearly depends on the laser amplitude (see the solid line), which is well known in nonlinear optics and can be understood from perturbation theory,^{8,17} i.e.,

$$\mathbf{P} = \alpha \mathbf{E} + \gamma \mathbf{E}\mathbf{E}\mathbf{E} + \dots, \quad (4)$$

where \mathbf{P} is the total polarization, \mathbf{E} is the electric field, and $\mathbf{E}\mathbf{E}\mathbf{E}$ denotes the tensor product,⁸ and α and γ are linear and

third-order polarizabilities, respectively. What is surprising is that when we increase τ , we find that the dependence changes substantially. For $\tau = 15$ fs, the increase is much sharper (see the dotted-line). Further increase in τ leads to a markedly higher-order increase, which is consistent with the experimental findings,⁷ but quickly the saturation starts at 0.15 eV/Å for $\tau = 20$ and 0.12 eV/Å for $\tau = 25$. Since it is difficult to systematically change the pulse duration experimentally, to the best of our knowledge, such observation has never been reported. The main reason for such dependence is because for a longer pulse duration, the system has a longer time to absorb the energy from the laser, thus allowing multiple excitations. For a given laser frequency, the number of states that the laser can access is limited even with multiple excitations taking place. This explains why the absorbed energy for a longer τ saturates at a relatively smaller field amplitude.

However, when we tune the laser frequency to the resonance $\omega = 2.37$ eV (corresponding to the first dipole-allowed transition from the HOMO to LUMO+1), a new story is revealed. First of all, as expected, on resonance the absorbed energy is much larger than that of off resonance. Second, although the major dependence of ΔE_{TOT} on the amplitude is similar to the off-resonance case, an increase in τ causes a dramatic effect of the laser intensity on the absorbed energy, where several shoulders and peaks appear. In particular, the first left shoulder, highlighted by the arrows, moves toward weaker field regions as the pulse width increases. What is remarkable is that for those larger τ 's, the absorbed energy starts to decrease and leaves a peak in the lower field region. This is most obvious for $\tau = 25$ fs, where the peak appears around 0.025 eV/Å. Such “darkening” is rather unexpected, but is similar to a hole burning process,⁸ where state bleaching is the underlying reason. The physical origin for the present darkening is complicated since, due to the Stark effect, the energy levels shift strongly. For instance, at $A = 0.025$ eV/Å, the gap between the E_{1g} and A_{2g} states is only about 0.004 eV, but at $A = 0.05$ eV/Å, it becomes 0.023 eV. In the meantime, the HOMO-LUMO+1 gap decreases with the field and introduces an earlier saturation, but the larger gap between E_{1g} and A_{2g} suppresses the continuous increase of the absorbed energy and leads to the darkening effect. This result is important for optical limiting applications.⁹ In particular, it shows that though an increase in the field amplitude generally increases the energy absorbed into the system, when operating at resonant frequencies, it is possible that less energy is effectively absorbed into the system as the field becomes stronger. This may present a new opportunity for future experimental research.

IV. CONCLUSION

In conclusion, by realistically including the laser field, we unfold a very rich picture of the ultrafast dynamics in C_{60} . Upon laser irradiation, the electron is initially excited out of the Fermi sea, and energy is mainly absorbed into the electron system. After the laser pulse is over, the lattice and the electron systems start to exchange energy periodically. De-

pending on the incident laser frequency, the absorbed energy exhibits a higher-order dependence on the field amplitude, which is consistent with the experimental results. Interestingly, on resonance the absorbed energy may decrease with an increase in the field amplitude. This may suggest a new way for future optical limiting applications.²⁸

ACKNOWLEDGMENTS

We would like to thank Dr. J. Dunn (Nottingham) and Professor H. Kroto (Sussex) for helpful communications. This work was in part supported by the National Science Foundation under NUE Proposal No. 0304487.

- ¹A.J. Heeger, *Rev. Mod. Phys.* **73**, 681 (2001).
- ²M.J. Rosker, H.O. Marcy, T.Y. Chang, J.T. Khoury, K. Hansen, and R.L. Whetten, *Chem. Phys. Lett.* **196**, 427 (1992); R.A. Cheville and N.J. Halas, *Phys. Rev. B* **45**, 4548 (1992); R. Jacquemin, S. Kraus, and W. Eberhardt, *Solid State Commun.* **105**, 449 (1998).
- ³S.L. Dexheimer, D.M. Mittleman, R.W. Schoenlein, W. Vareka, X.D. Xiang, A. Zettl, and C.V. Shank, *Springer Ser. Chem. Phys.* **55**, 81 (1993); S.B. Fleischer, E.P. Ippen, G. Dresselhaus, M.S. Dresselhaus, A.M. Rao, P. Zhou, and P.C. Eklund, *Appl. Phys. Lett.* **62**, 3241 (1993); V.M. Farztdinov, A.L. Dobryakov, V.S. Letokhov, Yu.E. Lozovik, Yu.A. Matveets, S.A. Kovalenko, and N.P. Ernsting, *Phys. Rev. B* **56**, 4176 (1997); see also J. Shinar, Z. V. Vardeny, and Z. H. Kafafi, *Optical and Electronic Properties of Fullerenes and Fullerene-Based Materials* (Marcel Dekker, New York, 2000).
- ⁴N.S. Sariciftci, L. Smilowitz, A.J. Heeger, and F. Wudl, *Science* **258**, 1474 (1992).
- ⁵Y. Wang, *Nature (London)* **356**, 585 (1992).
- ⁶G. Lanzani, *Synth. Met.* **111-112**, 493 (2000).
- ⁷Z.H. Kafafi, J.R. Lindle, R.G.S. Pong, F.J. Bartoli, L.J. Lingg, and J. Milliken, *Chem. Phys. Lett.* **188**, 492 (1992).
- ⁸Y. R. Shen, *The Principles of Nonlinear Optics* (Wiley, New York, 1984); R. W. Boyd, *Nonlinear Optics* (Academic Press, San Diego, 1992).
- ⁹L.W. Tutt and A. Kost, *Nature (London)* **356**, 225 (1992).
- ¹⁰W.N. Sisk, D.H. Kang, M.Y.A. Raja, and F. Farahi, *Int. J. Optoelectron.* **11**, 325 (1997).
- ¹¹H.A. Jahn and E. Teller, *Proc. R. Soc. London, Ser. A* **106**, 220 (1937); J.L. Dunn and C.A. Bates, *Phys. Rev. B* **52**, 5996 (1995); A. Ceulemans and P.W. Fowler, *J. Chem. Phys.* **93**, 1221 (1990).
- ¹²B. Friedman, *Phys. Rev. B* **45**, 1454 (1992); M.W. You, C.L. Wang, F.C. Zhang, and Z.B. Su, *ibid.* **47**, 4765 (1993); W.Z. Wang, Chui-Lin Wang, Zhao-Bin Su, and Lu Yu, *Phys. Rev. Lett.* **72**, 3550 (1994).
- ¹³M. Matus, H. Kuzmany, and E. Sohmen, *Phys. Rev. Lett.* **68**, 2822 (1992).
- ¹⁴G.P. Zhang, R.T. Fu, X. Sun, D.L. Lin, and T.F. George, *Phys. Rev. B* **50**, 11 976 (1994); X. Sun, G.P. Zhang, Y.S. Ma, R.L. Fu, X.C. Shen, K.H. Lee, Y.Y. Park, T.F. George, and L.N. Pandey, *ibid.* **53**, 15 481 (1996); G.P. Zhang, X. Sun, T.F. George, and L.N. Pandey, *J. Chem. Phys.* **106**, 6398 (1997).
- ¹⁵W.P. Su and J.R. Schrieffer, *Proc. Natl. Acad. Sci. U.S.A.* **77**, 5626 (1982).
- ¹⁶S.L. Dexheimer, W.A. Vareka, D. Mittleman, A. Zettl, and C.V. Shank, *Chem. Phys. Lett.* **235**, 552 (1995).
- ¹⁷G.P. Zhang, *Phys. Rev. Lett.* **86**, 2086 (2001).
- ¹⁸G.P. Zhang, T.A. Callcott, G.T. Woods, L. Lin, Brian Sales, D. Mandrus, and J. He, *Phys. Rev. Lett.* **88**, 077401 (2002); **88**, 189902(E) (2002).
- ¹⁹J. Bruening and B. Friedman, *J. Chem. Phys.* **106**, 9634 (1997).
- ²⁰G.P. Zhang and W. Hübner, *Phys. Rev. Lett.* **85**, 3025 (2000); G. P. Zhang, W. Hübner, E. Beaurepaire, and J.-Y. Bigot, in *Spin Dynamics in Confined Magnetic Structures I*, edited by B. Hillenbrand and K. Ounadjela (Springer, New York, 2002), p. 245 ff.
- ²¹Note that t measures the time of dynamics. Since in real experiments the laser pulse is not a simple delta function and has a finite width, we have to define (a) when the pulse reaches the maximum strength and (b) how long the pulse lasts. (a) is measured by t_0 and (b) is measured by τ . For instance, if $t_0=0$, then the pulse reaches the maximum at $t=0$. Therefore, all the negative time t means that the pulse hasn't reached the maximum. Depending on τ , ahead of this maximum the pulse may already appear. For example, if $\tau=10$ fs, then the laser field is nonzero from -10 fs to 10 fs. That is why at -8 fs we already have the laser field.
- ²²G.P. Zhang and T.F. George, *Phys. Rev. B* **66**, 033110 (2002).
- ²³We identify E_{1g} and A_{2g} states of T_{1g} and E_u and A_{1u} states of H_u by their degeneracies, but the assignment of E_{1u} and E_{2u} is based on whether the dipole transition to E_{1g} is allowed or not.
- ²⁴M. Lindberg and S.W. Koch, *Phys. Rev. B* **38**, 3342 (1988).
- ²⁵S. Datta, *Electronic Transport in Mesoscopic Systems* (Cambridge University Press, Cambridge, UK, 1995).
- ²⁶We do not expect that our model Hamiltonian could give a very accurate period since we do not include the bending and puckering terms.
- ²⁷A simple and quick way to see whether the oscillation is from the A_g mode is to check its frequency since most frequencies of the vibration modes in C₆₀ are known. The period of 67 fs corresponds to 497 cm⁻¹. By comparing this frequency against those frequencies, one can immediately find that this is the characteristic frequency of the A_g mode [see an excellent review article "Vibrational Spectroscopy of C₆₀," by J. Menendez and J. B. Page, in *Light Scattering in Solids VIII*, edited by M. Cardona and G. Güntherodt (Springer, Heidelberg, 2000)]. The normal mode analysis further confirms this assignment.
- ²⁸H.I. Elim, J. Ouyang, J. He, S.H. Goh, S.H. Tang, and W. Ji, *Chem. Phys. Lett.* **369**, 281 (2003).